TISSUE ENGINEERING: Part A
Volume 18, Numbers 19 and 20, 2012

DOI: 10.1089/ten.tea.2012.0475

A Murine Model of Volumetric Muscle Loss and a Regenerative Medicine Approach for Tissue Replacement

Brian M. Sicari, B.S.,[1,2] Vineet Agrawal, Ph.D.,[1,2] Bernard F. Siu, B.S.,[1] Christopher J. Medberry, B.S.,[1] Christopher L. Dearth, Ph.D.,[1] Neill J. Turner, Ph.D.,[1,3] and Stephen F. Badylak, D.V.M., M.D., Ph.D.[1,3]

Volumetric muscle loss (VML) resulting from traumatic accidents, tumor ablation, or degenerative disease is associated with limited treatment options and high morbidity. The lack of a reliable and reproducible animal model of VML has hindered the development of effective therapeutic strategies. The present study describes a critical-sized excisional defect within the mouse quadriceps muscle that results in an irrecoverable volumetric defect. This model of VML was used to evaluate the efficacy of a surgically placed inductive biologic scaffold material composed of porcine small intestinal submucosa–extracellular matrix (SIS-ECM). The targeted placement of an SIS-ECM scaffold within the defect was associated with constructive tissue remodeling including the formation of site-appropriate skeletal muscle tissue. The present study provides a reproducible animal model with which to study VML and shows the therapeutic potential of a bioscaffold-based regenerative medicine approach to VML.

Introduction

Adult skeletal muscle has robust inherent ability to regenerate in response to injury.[1–3] Skeletal muscle damage associated with crush injury or blunt trauma is typically associated with a host response that relies in large part upon the presence and activation of a myogenic stem cell population called satellite cells. Satellite cells possess the ability to exit quiescence, divide, migrate, and differentiate into myoblasts and then fuse into multinucleate muscle fibers.[4] The regenerative process has been described as occurring in three stages: a proliferative phase, the early differentiation stage, and the terminal differentiation stage. Each stage is regulated in part by the temporal expression of well-recognized muscle transcription factors of the basic helix-loop-helix family.[5] However, this regenerative response is critically dependent upon the type and severity of muscle insult.[4] When skeletal muscle injury is more severe and cannot be compensated via inherent regenerative mechanisms, the resulting irrecoverable loss of tissue is referred to as volumetric muscle loss (VML).[6]

Common causes of VML include military battlefield injuries,[7–9] civilian traumatic accidents, tumor ablation, or degenerative disease, and are associated with cosmetic and functional impairment. In the military setting, muscle trauma now accounts for between 50% and 70% of total war injuries with 80% of the surgical amputations performed on military casualties directly related to this missing tissue.[10,11] Therapeutic options for VML are very limited and include autologous tissue transfer, muscle transposition, or amputation with the implementation of prosthetic devices. These procedures, however, have yielded minimal success[12–14] and are associated with extensive donor site morbidity.[15,16] The lack of a reliable and easily reproducible animal model of VML has delayed the development of more effective treatment strategies.

Surgically placed biologic scaffolds composed of naturally occurring extracellular matrix (ECM) have been used to promote the site-appropriate constructive remodeling of soft tissue defects within the abdominal wall musculature,[17–20] musculotendinous junction,[21] esophagus,[22,23] and heart.[24] ECM-mediated constructive remodeling has been associated with enhanced functional myogenesis,[20] innervation,[25] and vascularization[17,18,20] within the remodeling scaffold. Therefore, scaffolds composed of ECM may provide a viable therapeutic approach for the clinical treatment of VML.

In the present study, a preclinical rodent model of VML that involved a unilateral excisional defect of the mouse quadriceps muscle was developed and evaluated. After 56 days, histologic examination revealed the defect to be of critical size and healed with dense collagenous scar tissue. Using this model, a bioscaffold-based regenerative medicine approach to VML treatment was evaluated.

[1]McGowan Institute for Regenerative Medicine, University of Pittsburgh, Pittsburgh, Pennsylvania.
Departments of [2]Pathology and [3]Surgery, University of Pittsburgh, Pittsburgh, Pennsylvania.

Materials and Methods

Overview of experimental design

Approval was obtained from the University of Pittsburgh Institutional Animal Care and Use Committee. Thirty-two female C57BL/6 mice were randomly assigned into either treated or untreated experimental groups. Both groups were subjected to a muscle defect consisting of unilateral resection of the tensor fascia latae quadriceps muscle. The defects within the treated group were filled with a biologic scaffold composed of porcine-derived small intestinal submucosa (SIS)-ECM. Nonresorbable marker sutures were placed at the corners of the defect in both groups and were used to identify the defect margins. The time points for evaluation were 7, 14, 28, and 56 days ($n=4$ per time point/group). Microscopic analysis included histochemistry and immunolabeling to examine skeletal muscle regeneration, vascularization, and innervation.

Scaffold preparation

The SIS-ECM material was prepared by decellularization of porcine jejunum using a combination of mechanical and chemical methods as previously described.[26] This material was then lyophilized and milled to produce particulate SIS with dimensions of 850 and 250 mm^2. This particulate SIS was combined in a ratio of 2:1, respectively, and vacuum pressed to form a powder pillow construct $25\times12.5\times3$ mm. This construct was cut into smaller pillows $4\times4\times3$ mm weighing approximately 27.6 ± 04.5 mg to be used as implants. Lyophilized SIS sheets (1 cm^2) were used to secure the pillows within the defect.

Surgical procedure

Female C57BL/6 mice, age 6–8 weeks, were purchased from Jackson Laboratories. Mice were anesthetized and maintained at a surgical plane of anesthesia with 1.5–2.5% isoflurane in oxygen and positioned in ventral recumbency. The surgical site was prepared in sterile fashion using a commercially available hair remover and 70% isopropyl alcohol followed by the placement of sterile drapes. A unilateral longitudinal incision measuring approximately 1.5 cm in length was made in the epidermis, dermis, and fascia to expose the underlying quadriceps compartment (Fig. 1A). After resection of a 4×3 mm full thickness segment of the tensor fasciae latae muscle along with a partial resection of the underlying rectus femoris, marker sutures (7-0 prolene, Ethicon, Inc.) were placed along the deep corners of the defect and anchored through the rectus femoris muscle (Fig. 1B). Sutures were placed to clearly identify the injury and/or implantation site at the time of tissue harvest. In the untreated group the most superficial edge of each defect was also marked by a simple interrupted suture. A minimal amount of suture material was placed only at the defect corners to avoid eliciting a host response to the suture that would obscure the host response to the injury alone. Defects in the treated group were filled with SIS-ECM powder pillows (Fig. 1C) and covered by a cubic centimeter of SIS-ECM sheet. The sheet was then sutured to the top edges of the defect in an interrupted fashion similar to the control (Fig. 1D). The entire sheet-pillow implant was hydrated using normal saline before dermal closure with 7-0 prolene in a continuous pattern. The wound was covered in betadine ointment after closure and assessed for signs of infection for 2 days postsurgery. Each mouse received Buprenex (buprenorphine hydrochloride, 0.25 mg/kg) for analgesia, and Baytril (enrofloxacin, 20 mg) an antibiotic, for 3 days postoperatively. All animals survived the surgical procedure and their predetermined study period without complications.

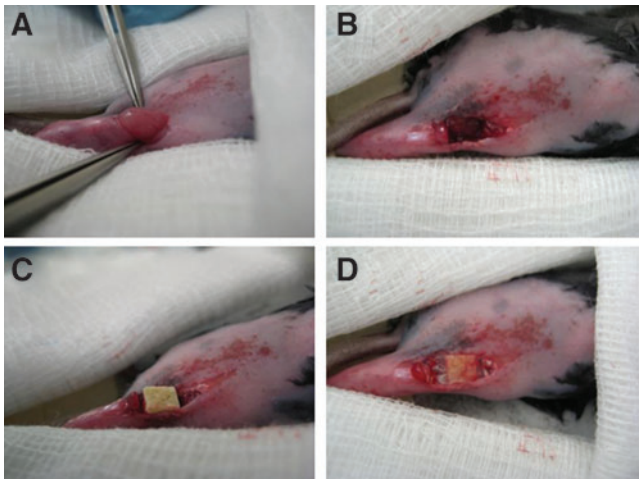

FIG. 1. Induction of VML injury. The exposed quadriceps muscle compartment after skin incision and blunt dissection of the surrounding fascia **(A).** Volumetric defect consisting of a 4×3 mm full-thickness resection of the tensor fasciae latae quadriceps muscle **(B).** Treated defect filled with a size-matched piece of vacuum-pressed SIS-ECM **(C).** Single-layer SIS-ECM sheet overlay sutured to adjacent native muscle before dermal closure **(D).** VML, volumetric muscle loss; SIS, small intestinal submucosa; ECM, extracellular matrix. Color images available online at www.liebertpub.com/tea

Specimen harvest and histology

Animals were sacrificed at 7, 14, 28, and 56 days. Each mouse was euthanized with 5% isoflurane in oxygen followed by an intracardiac injection of potassium chloride to induce cardiac arrest. The defect site and associated proximal and distal segment of the quadriceps muscles were isolated and surgically removed. The isolated tissue was either (1) flash-frozen in liquid nitrogen-cooled 2-methyl butane or (2) fixed in 10% neutral buffered formalin (NBF). Frozen tissues were embedded in frozen embedding media and cryosectioned into 8-μm-thick sagittal sections. NBF-fixed tissue was embedded in paraffin and cut into 5-μm-thick sagittal sections. All tissue sections were mounted onto glass slides for histologic staining (i.e., Masson's Trichrome) or for immunolabeling analysis.

Immunolabeling studies

Frozen tissue sections were fixed in ice cold 50:50 methanol:acetone for 5 min at room temperature and washed in phosphate-buffered saline (PBS). Tissue sections were blocked in blocking buffer (1% [w/v] bovine serum albumin/2% [v/v] normal horse serum/0.05% [v/v] Tween-20/0.05% [v/v] Triton X-100 in PBS) for 1 h to reduce nonspecific antibody binding. Tissue sections were then incubated in primary antibodies diluted in blocking buffer at 4°C for 16 h.

The primary antibodies used for the immunolabeling studies were (1) rabbit polyclonal CD31 (Abcam) on NBF fixed tissues at 1:200 dilution for identification of endothelial cells; (2) rabbit polyclonal Gap-43 (Abcam) on NBF fixed tissues at 1:200 for identification of neurons and; (3) monoclonal anti-desmin (Abcam) on frozen fixed tissues at 1:200 dilution for identification of muscle cells. After washing in PBS, tissue sections were incubated in fluorophore-conjugated secondary antibodies (Alexa Fluor® donkey anti-mouse or donkey anti-rabbit 488; Invitrogen). After washing again with PBS, nuclei were couterstained with 4′6-diamidino-2-phenylindole (DAPI) and slides were coated with anti-fade mounting media (Dako).

NBF-fixed tissues were deparaffinized with xylene and rehydrated through a graded ethanol series. Heat-mediated antigen retrieval was performed with 0.1 mM ethylenediaminetetraacetic acid buffer at 95–100°C for 25 min. After cooling for 15 min, enzyme-mediated antigen retrieval was performed with 0.1% (v/v) trypsin/0.1% (w/v) calcium chloride digestion at 37°C for 10 min. After washing in PBS tissue sections were blocked in blocking buffer for 1 h and incubated in primary antibodies at 4°C for 16 h. After additional PBS washing tissue sections were incubated in secondary antibodies for 1 h at room temperature, followed by DAPI nuclear stain before coverslipping. All tissue sections were imaged using a Zeiss Axio Observer Z1 or Nikon E600 microscope with Nuance multispectral imaging system (CRI, Inc.) with appropriate brightfield and fluorescent filter sets. Quantification of CD31-positive blood vessels was done by immunolabeling and counting the number of blood vessels per 400× field of view. Three images of each surgical site where quantified by two blinded independent investigators. Only positively labeled cells that were associated with a visible lumen were counted.

Statistical analysis

An independent Student's *t*-test was used to determine the differences in vascularity between SIS-ECM and no treatment at 7, 14, 28, and 56 days postinjury. All statistical analysis used SPSS Statistical Analysis Software (SPSS, IBM).

Results

Surgical procedures

All mice recovered from the surgical procedure without complications. The behavior and appetite of all subjects were unchanged after the procedure. No macroscopic abnormalities were noted at the time of removal of skin sutures (10–14 days after the procedure) or throughout the duration of the study.

Macroscopic and microscopic findings

Control group. Mice were allowed to heal for 56 days after surgical excision of a 4×3 mm full-thickness resection of the tensor fasciae latae and rectus femoris muscles in mouse quadriceps muscle. About 56 days postsurgery the volumetric defect remained and was easily identifiable by histologic methods (Fig. 2B, left panel, dotted line). The defect only experienced a mild flattening and associated deposition of a thin layer of disorganized, collagenous scar tissue (Fig. 2B, right panel). The persistence of a volumetric defect and

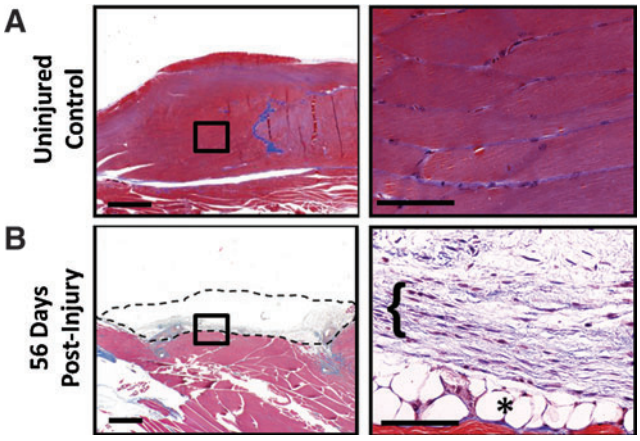

FIG. 2. VML injury is of critical size. Histological analysis of uninjured **(A)** and injured **(B)** muscle at 56 days postsurgery. After 56 days low-power magnification (left panels) reveals an obvious volumetric defect (dotted line). Higher magnification (right panels) shows the defect partially remodeled with a collagenous connective tissue consistent with scar formation ({) and some adipose (*). No signs of new skeletal muscle formation are seen in untreated injured muscle. The black boxes on the left represent the area of the high-power images on the right (scale bar = 1 mm). Color images available online at www.liebertpub.com/tea

deposition of collagenous connective tissue was consistent with a critical-sized defect, irrecoverable by the inherent endogenous regenerative potential of skeletal muscle. These results show that the VML injury model is of critical size and does not spontaneously heal.

The host response to untreated VML defects showed necrosis of skeletal muscle immediately surrounding the defect margins after 7 days (Fig. 3A, arrows). Neutrophils and

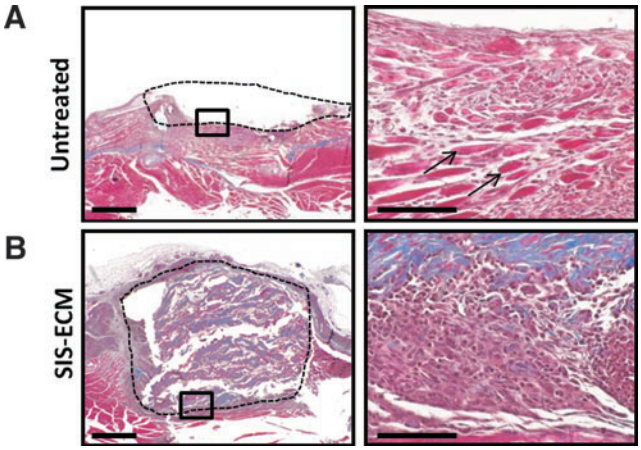

FIG. 3. Defect site at 7 days postsurgery. Low magnification (left panels) shows the defect site (dotted lines). Untreated defects **(A)** show a VML injury characterized by necrotic skeletal muscles (arrows), while treated defects **(B)** are filled with the SIS-ECM scaffold. High magnification (right panels) shows a robust mononuclear cell infiltrate in both untreated and treated defects. The black boxes on the left represent the area of the high magnification images on the right (scale bar = 1 mm). Color images available online at www.liebertpub.com/tea

mononuclear cells were present within the wound site at day 7. New blood vessels were present at day 7 and persisted through 28 days postsurgery (Fig. 6A, C). Gap-43+ nerve fibers were also observed around the defect margins at the interface with native muscle from days 7 to 28 postsurgery but did not extend into the defect site itself (Fig. 7A). By day 14, the defect site became partially filled with granulation tissue and the cells populating the defect site were predominantly mononuclear in morphology (Fig. 4A). By day 28 the cell population showed a marked decrease in number and host derived neomatrix could be identified along the margins of the defect site (Fig. 5A). After 56 days the untreated defects were characterized by dense partially organized connective tissue consistent with scar tissue formation within the injury site (Fig. 2B, right panel).

SIS-ECM-treated group. The host response to VML defects treated with an SIS-ECM scaffold was characterized by a dense infiltration of both neutrophils and mononuclear cells that surrounded the defect site and populated the outer edges of the scaffold at 7 days postsurgery, similar to untreated control groups (Fig. 3B). Angiogenesis was prominent at day 7 and remained a feature of the ECM-treated defect throughout the 56-day study period (Fig. 6B). Nerve fibers were present within the remodeling scaffold after 7 days and for the duration of the study period (Fig. 7B). After 14 days a uniformly distributed population of mononuclear cells populated the majority of the ECM scaffold (Fig. 4B). Host-derived neomatrix was intermingled with remnants of the ECM scaffold within the defect site. After 28 days, the majority of the ECM implant was cellularized, with the exception of a few areas within the center of the scaffold (Fig. 5B). Abundant neomatrix along with native skeletal muscle ingrowth could be identified along the scaffold margins. At 56 days postsurgery, the ECM scaffold was almost completely cellularized (Fig. 8A), showed islands of desmin+ cells along the interface with the underlying native muscle

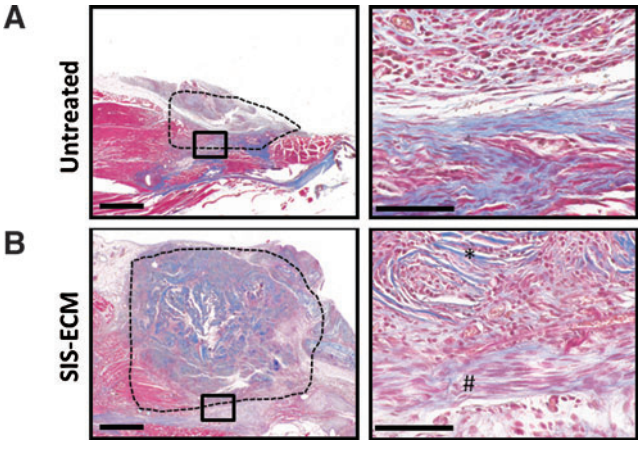

FIG. 4. Defect site at 14 days postsurgery. Low magnification (left panels) shows the defect site (dotted lines). Untreated defects are filling with granulation tissue, while the ECM scaffold is becoming infiltrated with cells. The black boxes on the left represent the area of the high magnification images on the right. (#, host derived neomatrix; *, scaffold) (scale bar = 1 mm). Color images available online at www.liebertpub.com/tea

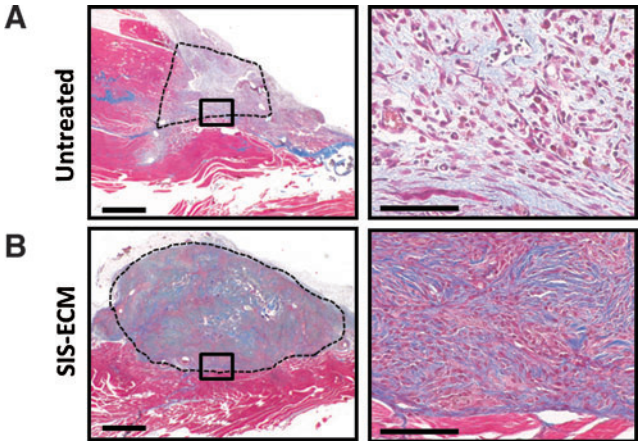

FIG. 5. Defect site at 28 days postsurgery. Low magnification (left panels) shows the defect site (dotted lines). High magnification (right panels) shows predominantly spindle-shaped cells populating the untreated defect site **(A)**, while treated defects are comprised of cells with varying morphologies **(B)**. The black boxes on the left represent the area of the high-magnification images on the right (scale bar = 1 mm). Color images available online at www.liebertpub.com/tea

(Fig. 8B, left panel), and was populated by islands of desmin+-striated skeletal muscle cells throughout (Fig. 8B, right panel).

Discussion

The present study describes a murine model of volumetric skeletal muscle injury that does not spontaneously heal. In addition, the findings of the present study showed that implantation of a biologic scaffold composed of ECM at the site of injury alters the default wound healing response from scar tissue deposition toward constructive remodeling, including the presence of new innervated and vascularized skeletal muscle.

Skeletal muscle has a robust capacity for regeneration after injury. The accepted paradigm of skeletal muscle regeneration is that quiescent satellite cells located beneath the basement membrane become activated and differentiate into new myotubes.[27–32] However, although debated, it is increasingly being recognized that there are additional progenitor cell populations that have the ability to form new muscle tissue.[33–37] Common rodent models used to experimentally induce skeletal muscle injury include cardiotoxin injection,[38] freezing,[39,40] and eccentric contraction-induced injury,[41,42] among others. Although these skeletal muscle injury models induce a significant amount of localized injury acutely, the tissue is typically able to be restored to native structure and function by the inherent regenerative capacity of skeletal muscle. Therefore, these canonical skeletal muscle injury models would be ineffective in studying potential VML therapies because of this spontaneous recovery. The present study describes a critical-sized volumetric muscle defect within an extremity, specifically within the quadriceps muscle compartment.

There are very limited therapeutic options for massive and overt loss of skeletal muscle tissue subsequent to trauma. Autologous muscle grafts or muscle transposition represent

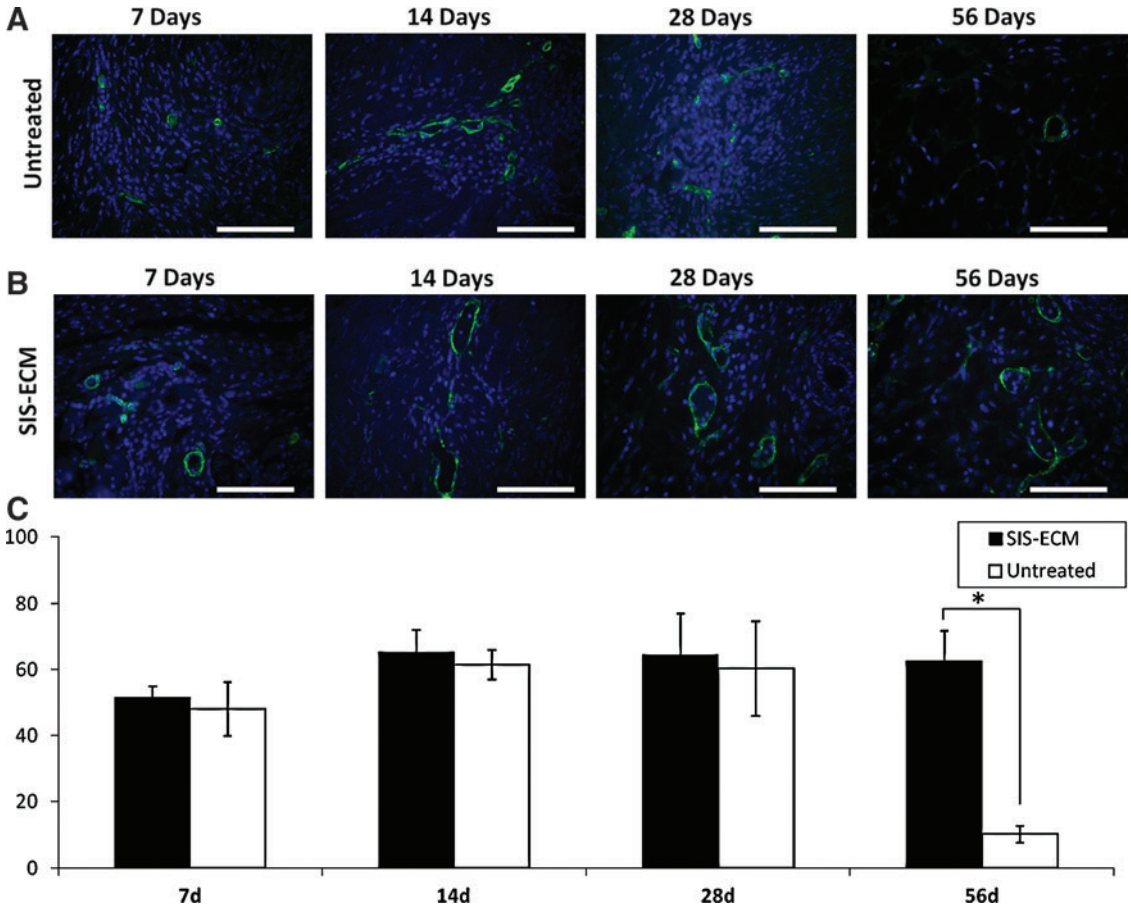

FIG. 6. Vascularity of treated versus untreated VML defects. CD31 staining (green) of endothelial cells at 7, 14, 28, and 56 days after VML in untreated defects **(A)** or defects treated with an SIS-ECM scaffold **(B).** CD31 immunopositive blood vessels were counted per 400× field of view **(C).** Three fields per surgical site were examined at the interface with underlying host tissue (*$p < 0.01$) (scale bar = 1 mm). (Error bars = standard deviation). Color images available online at www.liebertpub.com/tea

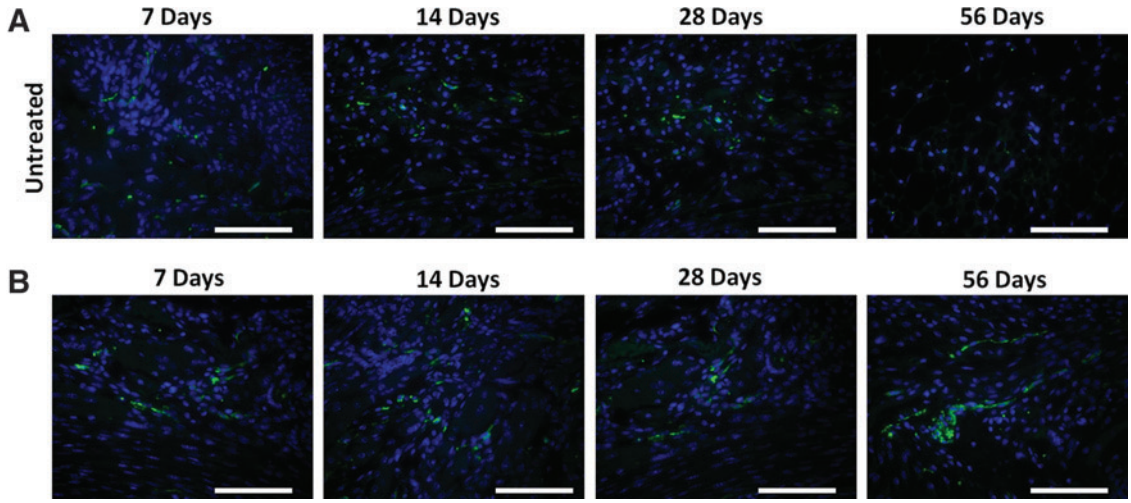

FIG. 7. Evidence of innervation within treated versus untreated VML defects. Representative images of Gap-43+ (green) neurons at 7, 14, 28, and 56 days after VML in untreated defects **(A)** or defects treated with an SIS-ECM scaffold **(B)** (scale bar = 1 mm). Color images available online at www.liebertpub.com/tea

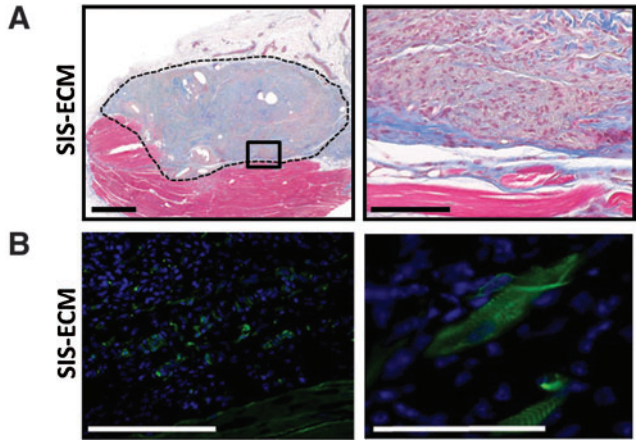

FIG. 8. Site-appropriate remodeling by ECM scaffolds. Defect sites treated with SIS-ECM (dotted line) maintain robust high cellularity after 56 days **(A).** Immunolabeling shows desmin+ cells (green staining) populating the area of ECM implantation along the interface of the underlying native muscle [**(B)**, left panel]. Desmin+-striated skeletal muscle cells were also observed throughout the SIS-ECM scaffold [**(B)**, right panel]. The black box on the left represents the area of the high magnification image on the right. Color images available online at www.liebertpub.com/tea

possible salvage procedures for restoration of absent muscle tissue but these approaches have limited success and are plagued by the associated morbidity at the donor site. Cell-based therapies are in their infancy and to date have been focused largely upon hereditary muscle disease such as Duchenne Muscular Dystrophy. There is an unequivocal need for regenerative medicine strategies that can enhance the innate regenerative ability of skeletal muscle after traumatic injury and/or induce *de novo* formation of functional muscle tissue due to congenital absence of such tissue. Development of a therapy that avoids the collection, isolation, and/or expansion and purification of autologous stem cells with subsequent re-introduction to the patient would almost certainly reduce the regulatory hurdles for clinical translation, reduce the cost of treatment, and avoid the risks associated with cell-based approaches.

Surgically placed biologic scaffolds composed of naturally occurring ECM have been used previously in preclinical studies to promote constructive remodeling of soft tissue defects.[21,43] Although such studies have not evaluated the ability of ECM scaffolds to promote constructive remodeling of volumetric muscle injuries, implantation of an ECM scaffold at a site of muscular injury resulted in deposition of site appropriate, functional muscle within 6 months post-implantation.[20] The mechanisms underlying this process are not well understood; however, rapid angiogenesis, degradation of the ECM scaffold, recruitment of differentiated and progenitor cells, and local modulation of the immune response are all logical and plausible factors that contribute to ECM-mediated remodeling of muscular tissue.[25,43–45]

Previous studies have shown that cells that accumulate at a site of ECM implantation include macrophages,[19,46] multipotential stem/progenitor cells,[47,48] endothelial cells,[49,50] nerves,[25] and muscle cells.[20] The temporal appearance of these cell phenotypes is likely dependent upon anatomic site,[45] microenvironmental niche factors,[51] and epigenetic factors such as mechanical forces.[52] Degradation products of ECM scaffolds have been shown to include chemotactic factors for myogenic progenitor cells.[47,53,54] Thus, it is possible that a subset of the dense mononuclear cells includes progenitor cells with myogenic potential. Future studies will further investigate the spatial and temporal pattern of accumulation of various myogenic progenitor cells after implantation of an ECM scaffold at a site of volumetric muscular injury.

Site-appropriate and constructive remodeling after a traumatic VML injury would intuitively be associated with a robust cellular response including prolonged angiogenesis and neurogenesis. The present study shows that after injury, ECM treated and untreated VML defects are both characterized by a robust mononuclear response consisting of many different cell types, including endothelial and nerve cells at 7–28 days postinjury. However, these treated versus untreated injury responses are dissimilar at 56 days post-injury. After 56 days the ECM-treated defects continue to show angiogenesis, the presence of nerves, and a diffuse cellular infiltrate that includes desmin+-striated skeletal muscle cells. In contrast, at 56 days postinjury, untreated defects show a response consistent with default wound healing and scar formation including a decreased cellular infiltrate and no signs of angiogenesis, innervation, or skeletal muscle. This murine model represents a useful tool for studying potential VML therapies.

The present study developed a mouse model of VML and evaluated a bio-scaffold-based regenerative medicine approach for site-specific tissue replacement. However, there are limitations that must be noted in the interpretation of the data. First, the results represent remodeling outcomes up to 56 days postinjury. Although desmin+-striated skeletal muscle cells were populating the scaffold implantation site, future studies of longer duration will prove if these cells have the capability to fuse and span the length of the defect. Second, the present study is lacking functional testing. Future studies examining the extent of functional recovery after a longer study period are warranted and in progress.

In conclusion, the present study describes a model of volumetric muscle injury that does not spontaneously heal. The placement of an ECM scaffold at the site of injury results in a significant deviation from the default response of scar tissue deposition toward a more constructive remodeling outcome, including the formation of desmin+ islands of muscle within the ECM construct. Although the mechanisms underlying this process are not yet fully understood, the development of a murine model allows for a more sophisticated and in-depth investigation of potential mechanisms by which ECM scaffolds promote constructive remodeling. Future studies may utilize transgenic mice and lineage tracing to definitively determine the role that progenitor cells play in ECM-mediated constructive remodeling.

Disclosure Statement

No competing financial interests exist.

References

1. Mauro, A. Satellite cell of skeletal muscle fibers. J Biophys Biochem Cytol **9,** 493, 1961.

2. Muir, A.R., Kanji, A.H., and Allbrook, D. The structure of the satellite cells in skeletal muscle. J Anat **99,** 435, 1965.
3. Charge, S.B., and Rudnicki, M.A. Cellular and molecular regulation of muscle regeneration. Physiol Rev **84,** 209, 2004.
4. Hill, M., Wernig, A., and Goldspink, G. Muscle satellite (stem) cell activation during local tissue injury and repair. J Anat **203,** 89, 2003.
5. Adair-Kirk, T.L., Atkinson, J.J., Kelley, D.G., Arch, R.H., Miner, J.H., and Senior, R.M. A chemotactic peptide from laminin alpha 5 functions as a regulator of inflammatory immune responses via TNF alpha-mediated signaling. J Immunol **174,** 1621, 2005.
6. Grogan, B.F., and Hsu, J.R. Volumetric muscle loss. J Am Acad Orthop Surg.**19 Suppl 1,** S35, 2011.
7. Lew, T.A., Walker, J.A., Wenke, J.C., Blackbourne, L.H., and Hale, R.G. Characterization of craniomaxillofacial battle injuries sustained by United States service members in the current conflicts of Iraq and Afghanistan. J Oral Maxillofac Surg **68,** 3, 2010.
8. Mazurek, M.T., and Ficke, J.R. The scope of wounds encountered in casualties from the global war on terrorism: from the battlefield to the tertiary treatment facility. J Am Acad Orthop Surg **14,** S18, 2006.
9. Owens, B.D., Kragh, J.F., Jr., Wenke, J.C., Macaitis, J., Wade, C.E., and Holcomb, J.B. Combat wounds in operation Iraqi Freedom and operation Enduring Freedom. J Trauma **64,** 295, 2008.
10. Mannion, S.J., and Chaloner, E. Principles of war surgery. BMJ **330,** 1498, 2005.
11. Bowyer, G. Debridement of extremity war wounds. J Am Acad Orthop Surg **14,** S52, 2006.
12. Lin, S.H., Chuang, D.C., Hattori, Y., and Chen, H.C. Traumatic major muscle loss in the upper extremity: reconstruction using functioning free muscle transplantation. J Reconstr Microsurg **20,** 227, 2004.
13. Fan, C., Jiang, P., Fu, L., Cai, P., Sun, L., and Zeng, B. Functional reconstruction of traumatic loss of flexors in forearm with gastrocnemius myocutaneous flap transfer. Microsurgery **28,** 71, 2008.
14. Vekris, M.D., Beris, A.E., Lykissas, M.G., Korompilias, A.V., Vekris, A.D., and Soucacos, P.N. Restoration of elbow function in severe brachial plexus paralysis via muscle transfers. Injury **39 Suppl 3,** S15, 2008.
15. Deutinger, M., Kuzbari, R., Paternostro-Sluga, T., Quittan, M., Zauner-Dungl, A., Worseg, A., *et al.* Donor-site morbidity of the gracilis flap. Plast Reconstr Surg **95,** 1240, 1995.
16. Kimata, Y., Uchiyama, K., Ebihara, S., Sakuraba, M., Iida, H., Nakatsuka, T., *et al.* Anterolateral thigh flap donor-site complications and morbidity. Plast Reconstr Surg **106,** 584, 2000.
17. Badylak, S., Kokini, K., Tullius, B., Simmons-Byrd, A., and Morff, R. Morphologic study of small intestinal submucosa as a body wall repair device. J Surg Res **103,** 190, 2002.
18. Clarke, K.M., Lantz, G.C., Salisbury, S.K., Badylak, S.F., Hiles, M.C., and Voytik, S.L. Intestine submucosa and polypropylene mesh for abdominal wall repair in dogs. J Surg Res **60,** 107, 1996.
19. Brown, B.N., Valentin, J.E., Stewart-Akers, A.M., McCabe, G.P., and Badylak, S.F. Macrophage phenotype and remodeling outcomes in response to biologic scaffolds with and without a cellular component. Biomaterials **30,** 1482, 2009.
20. Valentin, J.E., Turner, N.J., Gilbert, T.W., and Badylak, S.F. Functional skeletal muscle formation with a biologic scaffold. Biomaterials **31,** 7475, 2010.
21. Turner, N.J., Yates, A.J., Jr., Weber, D.J., Qureshi, I.R., Stolz, D.B., Gilbert, T.W., *et al.* Xenogeneic extracellular matrix as an inductive scaffold for regeneration of a functioning musculotendinous junction. Tissue Eng Part A **16,** 3309, 2010.
22. Nieponice, A., McGrath, K., Qureshi, I., Beckman, E.J., Luketich, J.D., Gilbert, T.W., *et al.* An extracellular matrix scaffold for esophageal stricture prevention after circumferential EMR. Gastrointest Endosc **69,** 289, 2009.
23. Badylak, S.F., Vorp, D.A., Spievack, A.R., Simmons-Byrd, A., Hanke, J., Freytes, D.O., *et al.* Esophageal reconstruction with ECM and muscle tissue in a dog model. J Surg Res **128,** 87, 2005.
24. Kelly, D.J., Rosen, A.B., Schuldt, A.J., Kochupura, P.V., Doronin, S.V., Potapova, I.A., *et al.* Increased myocyte content and mechanical function within a tissue-engineered myocardial patch following implantation. Tissue Eng Part A **15,** 2189, 2009.
25. Agrawal, V., Brown, B.N., Beattie, A.J., Gilbert, T.W., and Badylak, S.F. Evidence of innervation following extracellular matrix scaffold-mediated remodelling of muscular tissues. J Tissue Eng Regen Med **3,** 590, 2009.
26. Freytes, D.O., Badylak, S.F., Webster, T.J., Geddes, L.A., and Rundell, A.E. Biaxial strength of multilaminated extracellular matrix scaffolds. Biomaterials **25,** 2353, 2004.
27. Kitzmann, M., Carnac, G., Vandromme, M., Primig, M., Lamb, N.J., and Fernandez, A. The muscle regulatory factors MyoD and myf-5 undergo distinct cell cycle-specific expression in muscle cells. J Cell Biol **142,** 1447, 1998.
28. Collins, C.A., Olsen, I., Zammit, P.S., Heslop, L., Petrie, A., Partridge, T.A., *et al.* Stem cell function, self-renewal, and behavioral heterogeneity of cells from the adult muscle satellite cell niche. Cell **122,** 289, 2005.
29. Rantanen, J., Hurme, T., Lukka, R., Heino, J., and Kalimo, H. Satellite cell proliferation and the expression of myogenin and desmin in regenerating skeletal muscle: evidence for two different populations of satellite cells. Lab Invest **72,** 341, 1995.
30. Hawke, T.J., and Garry, D.J. Myogenic satellite cells: physiology to molecular biology. J Appl Physiol **91,** 534, 2001.
31. Dhawan, J., and Rando, T.A. Stem cells in postnatal myogenesis: molecular mechanisms of satellite cell quiescence, activation and replenishment. Trends Cell Biol **15,** 666, 2005.
32. Olguin, H.C., and Olwin, B.B. Pax-7 up-regulation inhibits myogenesis and cell cycle progression in satellite cells: a potential mechanism for self-renewal. Dev Biol **275,** 375, 2004.
33. Sun, D., Martinez, C.O., Ochoa, O., Ruiz-Willhite, L., Bonilla, J.R., Centonze, V.E., *et al.* Bone marrow-derived cell regulation of skeletal muscle regeneration. FASEB J **23,** 382, 2009.
34. Ferrari, G., Cusella-De Angelis, G., Coletta, M., Paolucci, E., Stornaiuolo, A., Cossu, G., *et al.* Muscle regeneration by bone marrow-derived myogenic progenitors. Science **279,** 1528, 1998.
35. de la Garza-Rodea, A.S., van der Velde, I., Boersma, H., Goncalves, M.A., van Bekkum, D.W., de Vries, A.A., *et al.* Long-term contribution of human bone marrow mesenchymal stromal cells to skeletal muscle regeneration in mice. Cell Transplant **20,** 217, 2011.
36. Drapeau, C., Antarr, D., Ma, H., Yang, Z., Tang, L., Hoffman, R.M., *et al.* Mobilization of bone marrow stem cells with stem enhance improves muscle regeneration in cardiotoxin-induced muscle injury. Cell Cycle **9,** 1819, 2010.
37. Ojima, K., Uezumi, A., Miyoshi, H., Masuda. S., Morita, Y., Fukase, A., *et al.* Mac-1(low) early myeloid cells in the bone

marrow-derived SP fraction migrate into injured skeletal muscle and participate in muscle regeneration. Biochem Biophys Res Commun **321,** 1050, 2004.
38. Couteaux, R., Mira, J.C., and d'Albis, A. Regeneration of muscles after cardiotoxin injury. I. Cytological aspects. Biol Cell **62,** 171, 1988.
39. Price, H.M., Howes, E.L., Jr., and Blumberg, J.M. Ultrastructural alterations in skeletal muscle fibers injured by cold. Ii. Cells on the sarcolemmal tube: observations on "Discontinuous" regeneration and myofibril formation. Lab Invest **13,** 1279, 1964.
40. Conboy, I.M., Conboy, M.J., Smythe, G.M., and Rando, T.A. Notch-mediated restoration of regenerative potential to aged muscle. Science **302,** 1575, 2003.
41. Warren, G.L., Ingalls, C.P., Shah, S.J., and Armstrong, R.B. Uncoupling of *in vivo* torque production from EMG in mouse muscles injured by eccentric contractions. J Physiol **515 (Pt 2),** 609, 1999.
42. Lowe, D.A., Warren, G.L., Ingalls, C.P., Boorstein, D.B., and Armstrong, R.B. Muscle function and protein metabolism after initiation of eccentric contraction-induced injury. J Appl Physiol **79,** 1260, 1995.
43. Valentin, J.E., Badylak, J.S., McCabe, G.P., and Badylak, S.F. Extracellular matrix bioscaffolds for orthopaedic applications. A comparative histologic study. J Bone Joint Surg Am **88,** 2673, 2006.
44. Badylak, S.F., and Gilbert, T.W. Immune response to biologic scaffold materials. Semin Immunol **20,** 109, 2008.
45. Badylak, S.F. The extracellular matrix as a biologic scaffold material. Biomaterials **28,** 3587, 2007.
46. Badylak, S.F., Valentin, J.E., Ravindra, A.K., McCabe, G.P., and Stewart-Akers, A.M. Macrophage phenotype as a determinant of biologic scaffold remodeling. Tissue Eng Part A **14,** 1835, 2008.
47. Agrawal, V., Johnson, S.A., Reing, J., Zhang, L., Tottey, S., Wang, G., *et al.* Epimorphic regeneration approach to tissue replacement in adult mammals. Proc Natl Acad Sci U S A **107,** 3351, 2010.
48. Agrawal, V., Tottey, S., Johnson, S.A., Freund, J.M., Siu. B.F., and Badylak. S.F. Recruitment of progenitor cells by an extracellular matrix cryptic peptide in a mouse model of digit amputation. Tissue Eng Part A **17,** 2435, 2011.
49. Reing, J.E., Zhang, L., Myers-Irvin, J., Cordero, K.E., Freytes, D.O., Heber-Katz, E., *et al.* Degradation products of extracellular matrix affect cell migration and proliferation. Tissue Eng Part A **15,** 605, 2009.
50. Vorotnikova, E., McIntosh, D., Dewilde, A., Zhang, J., Reing, J.E., Zhang, L., *et al.* Extracellular matrix-derived products modulate endothelial and progenitor cell migration and proliferation *in vitro* and stimulate regenerative healing *in vivo*. Matrix Biol **29,** 690, 2010.
51. Badylak, S.F., Freytes, D.O., and Gilbert, T.W. Extracellular matrix as a biological scaffold material: structure and function. Acta Biomater **5,** 1, 2009.
52. Boruch, A.V., Nieponice, A., Qureshi, I.R., Gilbert, T.W., and Badylak, S.F. Constructive remodeling of biologic scaffolds is dependent on early exposure to physiologic bladder filling in a canine partial cystectomy model. J Surg Res **161,** 217, 2010.
53. Crisan, M., Yap, S., Casteilla, L., Chen, C.W., Corselli, M., Park, T.S., *et al.* A perivascular origin for mesenchymal stem cells in multiple human organs. Cell Stem Cell **3,** 301, 2008.
54. Tottey, S., Corselli, M., Jeffries, E.M., Londono, R., Peault, B., and Badylak, S.F. Extracellular matrix degradation products and low-oxygen conditions enhance the regenerative potential of perivascular stem cells. Tissue Eng Part A **17,** 37, 2011.

Address correspondence to:
Stephen F. Badylak, D.V.M., M.D., Ph.D.
McGowan Institute for Regenerative Medicine
University of Pittsburgh
Bridgeside Point 2 Building
450 Technology Drive, Suite 300
Pittsburgh, PA 15213

E-mail: badylaks@upmc.edu

Received: August 3, 2011
Accepted: August 6, 2012
Online Publication Date: September 25, 2012